Inorganic Chemistry

pubs.acs.org/IC

Communication

Tuning the Equatorial Crystal-Field in Mononuclear Dy^{III} Complexes to Improve Single-Molecule Magnetic Properties

Li Zhu, Bing Yin,* Pengtao Ma, and Dongfeng Li*

Cite This: https://dx.doi.org/10.1021/acs.inorgchem.0c01716

Read Online

ACCESS | Metrics & More | Article Recommendations | Supporting Information

ABSTRACT: Two Dy^{III} complexes, [Dy(bbpen-F)X] [X = Cl (**1**), Br (**2**); H_2bbpen-F = *N*,*N*′-bis(2-hydroxybenzyl)-*N*,*N*′-bis(5-fluoro-2-methylpyridyl)ethylenediamine], have been synthesized that show remarkable single-molecule-magnet behavior with effective barriers of magnetic reversal of 837.7 K for **1** and 1149.7 K for **2** under zero direct-current field and hysteresis loops up to 20 K for **1** and 30 K for **2**, as confirmed by magnetic properties and ab initio calculations.

In the preceding years, single-molecule magnets (SMMs) have had potential applications in the fields of molecular spintronics, quantum computing, and high-density information storage materials[1−3] because of their large effective energy barrier (U_{eff}) and high blocking temperature (T_B),[4] while Ln ions have huge magnetic anisotropy, large magnetic moments, and strong spin−orbit coupling,[5,6] which make them attractive candidates for the preparation of high-performance SMMs. Therefore, Ln-SMMs have aroused the interest of many researchers, and mononuclear Ln-SMMs[7−31] have highly contributed because the interion coupling is usually negligible. Theoretical studies have shown that, to increase U_{eff} and T_B of a Dy-SMM, one needs to supply a coordination environment providing a very strong axial crystal-field component (electrostatic field) and a weak equatorial electrostatic field.[12,15,22a,28a]

High-order symmetries such as C_{∞}, D_{5h}, and D_{4d} are very important for the restraint of quantum tunneling of magnetization (QTM) because the splitting is forced to be zero in these ideal symmetries.[17c,d,23,25,29a] As reported, many Ln-SMMs with high symmetry have been synthesized, but only a very small part of them have U_{eff} and T_B above 1000 and 20 K,[7b,11,17a,18a−c,19a,13a,b] respectively (see Table S1 for a detailed list of these complexes).

It is worth mentioning that Tong's group reported the first SMM with pentagonal-bipyramidal (PBP) geometry (D_{5h}) in 2013.[17c] Later on, they utilized a hexadentate ligand, *N*,*N*′-bis(2-hydroxybenzyl)-*N*,*N*′-bis(2-methylpyridyl)-ethylenediamine (H_2bbpen), to obtain the first Dy-SMM possessing U_{eff} over 1000 K and T_B around 20 K with PBP geometry.[17a] Although current records of the highest U_{eff}(2218 K) and T_B(80 K) are held by a sandwich Dy^{III} compound,[7b] the works of Tong's group are still highly attractive because of the fact that the obtained crystals are solvent-free and stable in the air. It should be reasonable to believe that the solvent-free and stable complexes can minimize the possibility of giving rise to complex behaviors because of decomposition and/or distortion of the structure.[17a]

So far, more efforts have been made to amend the anisotropy of Ln^{III} ions in enhancing the axial electrostatic field; however, few studies have been reported on the weakening of the equatorial electrostatic field, which could also have a remarkable effect on the SMM behavior.[22b,24,28b,30] The Dy^{III} sandwich system has shown enormous success in enhancing the axial electrostatic field and weakening the equatorial electrostatic field at the same time.[7b] For the stable Tong PBP Dy^{III} compound,[17a] according to our best knowledge, only one work has been reported to date in which the axial positions of the ligand (phenol groups) are modified with the electron-donating methyl groups to give a new Dy^{III} complex with increased U_{eff} and T_B. No effort has been reported to modify the equatorial pyridyl groups of the H_2bbpen ligand to improve the SMM behavior in this system.

Here, we tried to introduce electron-withdrawing groups, e.g., an F atom, to the equatorial pyridyl groups, which will reduce the amount of negative charge of the coordinating pyridyl N atoms located on the equatorial positions of the coordination sphere. We propose that it will produce a weaker equatorial electrostatic field to give better SMM behavior. Following up with this idea, we synthesized a new ligand H_2bbpen-F with F atoms at the equatorial pyridyl groups and obtained two corresponding air-stable PBP Dy^{III} complexes, of which the structures and magnetic properties were researched.

Upon the reaction of H_2bbpen-F with DyX_3 and triethylamine using acetonitrile as the solvent, well-shaped block crystals [Dy(bbpen-F)X] [X = Cl (**1**), Br (**2**)] were obtained under solvothermal conditions. Single-crystal X-ray diffraction analysis (Tables S2 and S3) indicates that two complexes crystallize in the orthorhombic crystal system with a *Pbcn* space group. The structures of the two complexes contain a Dy^{III} ion, a bbpen-F^{2-} ligand, and Cl^- or Br^- (Figures 1 and S1−S3).

The center Dy^{III} locations in complexes **1** and **2** have distorted PBP coordination geometry (Table S4) formed by

Received: June 10, 2020

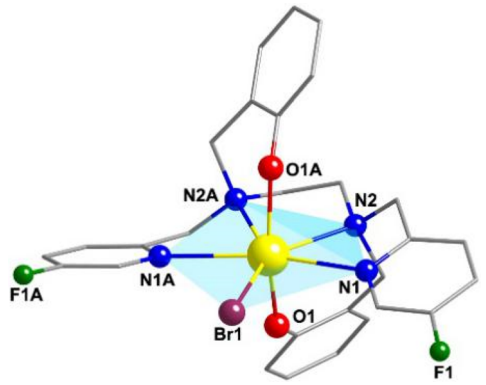

Figure 1. Crystal structure of **2**. H atoms are omitted for clarity. Color code: Dy, yellow; Br, plum; O, red; N, blue; C, gray. A = $-x + 2, y, -z + {}^{3}/_{2}$.

two O and four N atoms of a bbpen-F^{2-} ligand and one Br (Cl) atom of $DyBr_3$ ($DyCl_3$). In the axial direction, the two negatively charged O atoms of phenol are coordinated to Dy^{III} with the rather short Dy1−O1 bond lengths of **1** and **2**, 2.160(2) and 2.155(2) Å, respectively. Also, the O1−Dy1−O1A bond angles of **1** and **2** are 156.82(13)° and 157.52(11)°, respectively. In the equatorial direction, the four N atoms and one Br (Cl) atom formed five coordination sites through an average Dy−N bond length of 2.581 Å for **2** (2.576 Å for **1**) and a long Dy1−Br1 (Dy1−Cl1) distance of 2.8462(6) Å for **2** [2.6680 (14) Å for **1**; Table S3]. The closest intermolecular distance between two Dy^{III} ions is 8.502 Å for **1** and 8.549 Å for **2** (Figure S2 and Table S5). The structures are very similar to Tong's complexes,[17a] and the specific bond lengths and angles of these complexes are shown in Table S6 for comparison.

Temperature-dependent magnetic susceptibility experiments were fulfilled on polycrystalline samples of these complexes under a 1000 Oe external field and the temperature range 300−2 K. The values of $\chi_M T$ are 14.00 and 13.81 $cm^3 \cdot K \cdot mol^{-1}$ for **1** and **2** at room temperature, respectively (Figure S4). The $\chi_M T$ values of complexes **1** and **2** are in accordance with the theoretical value ($J = {}^{15}/_{2}$, $g = {}^{4}/_{3}$, 14.17 $cm^3 \cdot K\ mol^{-1}$) for one magnetically separated Dy^{III} ion. Along with the temperature drops, the $\chi_M T$ value also decreases marginally, and then it dramatically drops at low temperature and reaches the values of 6.77 $cm^3 \cdot mol^{-1} \cdot K$ (for **1**) and 4.01 $cm^3 \cdot mol^{-1} \cdot K$ (for **2**) at 2 K, strongly implying the presence of crystal-field splitting with separated excited-state Kramers doublets. The field dependent on the magnetization of **1** and **2** was measured from the zero direct-current (dc) field to 70 kOe at 2.0 K (Figure S5). The magnetization values achieved are respectively 5.25 and 4.98 $N\mu_B$ for **1** and **2** at 70 kOe, which are lower than the theoretical saturation value of 10 $N\mu_B$. Unsaturation of magnetization was probably a result of the crystal-field effects, low-lying excited states, and/or existence of significant magnetic anisotropy.[19b,22c,31]

To deeply investigate the SMM behavior in **1** and **2**, the blocking of magnetization and field-dependent magnetization measurements were conducted with an average sweep rate of 200 $Oe \cdot s^{-1}$ and a field range of −3 to +3 T under different temperatures (Figure 2). Butterfly-shaped magnetic hysteresis loops are obviously open at 20 K for **1** and at 30 K for **2** under zero dc field, which are due to the slow relaxation time for the complexes. By a comparison with T_B in Tong's work,[17a] **1** and

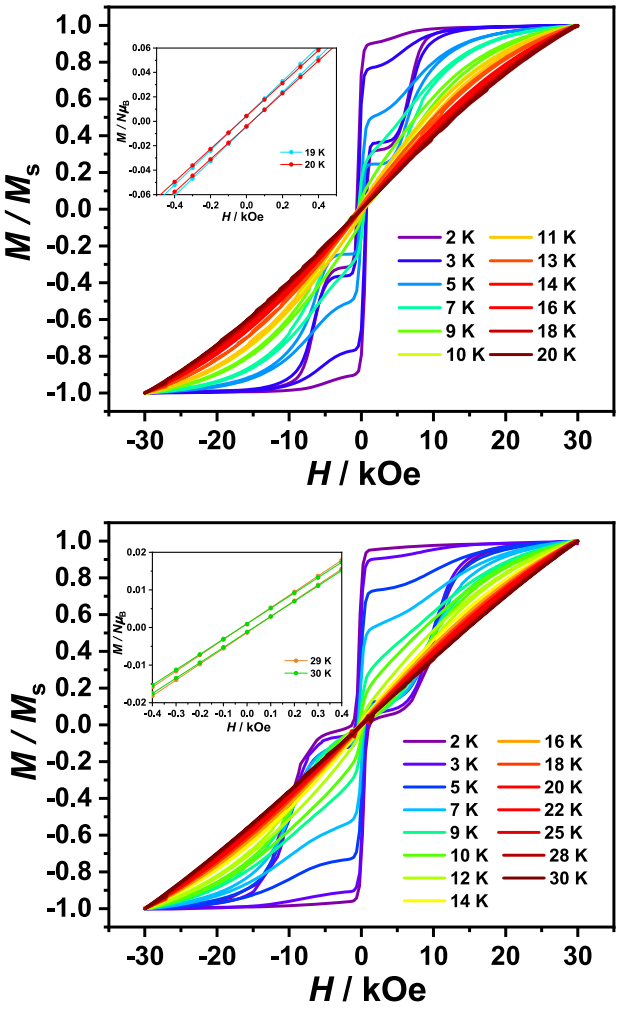

Figure 2. Magnetic hysteresis loops of **1** (top) and **2** (bottom) with a 200 $Oe \cdot s^{-1}$ sweep rate. Insets: Zoomed-in hysteresis loops at 19−20 K for **1** (29−30 K for **2**) with a 20 $Oe \cdot s^{-1}$ sweep rate.

2 show higher T_B than [Dy(bbpen)Br], indicating improvement in the SMM properties of the two complexes. To better investigate the dynamics of the magnetic properties, alternating-current (ac) susceptibility calculations were carried out at temperature dependences in zero dc and 2.5 Oe ac fields for complexes **1** and **2**. Complexes **1** and **2** display obvious temperature dependencies for out-of-phase susceptibility (χ''), the peaks of which are in good shape, demonstrating typical SMM behaviors (Figures S6 and S7). Besides, the frequency dependencies on the ac susceptibility measurements were performed under zero dc field to analyze the dynamics of the magnetic properties for **1** and **2**. The data show typical slow magnetic relaxation behavior (Figures 3 and S8−S11).

In order to explore the relaxation process, the Cole−Cole curves were studied at variable temperatures for complexes **1** and **2** (Figures S12−S15 and Tables S7 and S8). These curves obey a generalized Debye model, with the distribution of relaxation time (α) parameters in the region 0.00−0.02 between 35 and 60 K for **1** and in the region 0.02−0.04 between 30 and 58 K for **2**. The small distribution coefficient α values show that there is a narrow distribution of relaxation time for the magnetic relaxations of **1** and **2**.

The derived $\ln(\tau)$ versus T^{-1} plots for complexes **1** and **2** show that the Orbach process is the main process at high

https://dx.doi.org/10.1021/acs.inorgchem.0c01716
Inorg. Chem. XXXX, XXX, XXX−XXX

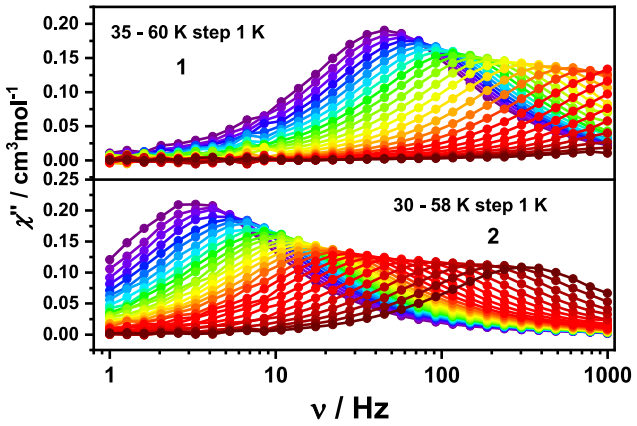

Figure 3. Frequency dependencies of the out-of-phase ac susceptibility for **1** (top) and **2** (bottom) in zero external field and at the indicated temperatures.

temperature, in which the fitting of the Arrhenius formula $\tau = \tau_0 \exp(U_{eff}/k_BT)$ gives U_{eff}/k_B = 827.9 K and $\tau_0 = 1.5 \times 10^{-11}$ s for **1** and U_{eff}/k_B = 1042.3 K and $\tau_0 = 7.6 \times 10^{-12}$ s for **2** (Figure 4), while at low temperature, other possible relaxation processes become competitive. Thus, the $\ln(\tau)$ versus T^{-1} curve of **1** is fitted with eq 1,[16,26,29b] which yields $\tau_0 = 1.4 \times 10^{-11}$ s, τ_{QTM} = 0.16 s, U_{eff}/k_B = 837.7 K, $C = 2.1 \times 10^{-3}$ $s^{-1}\cdot K^{-3.3}$, and n = 3.3.

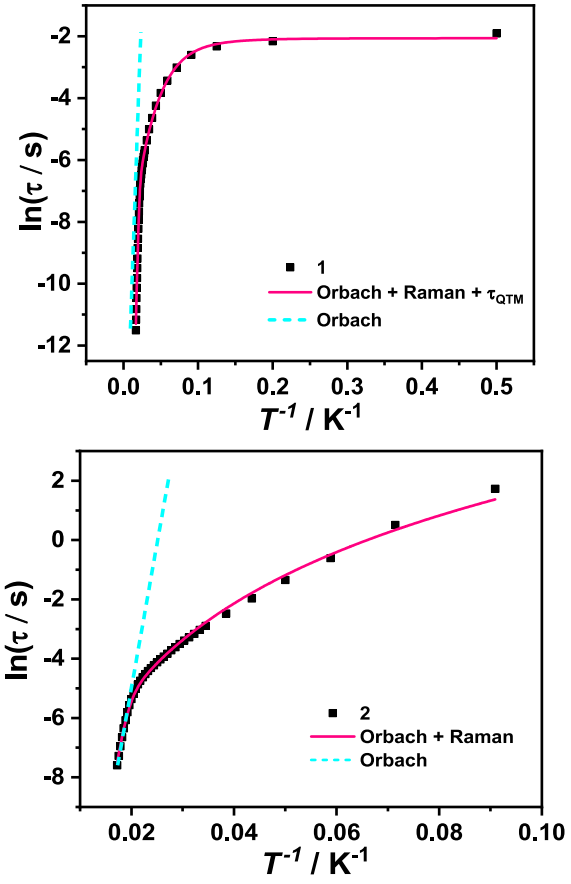

Figure 4. $\ln(\tau)$ versus T^{-1} plots at 0 Oe for **1** (top) and **2** (bottom). The cyan dashed line and pink solid line represent part of the Orbach process and the best fitting to the multiple relaxation process, respectively (see the text for the details).

$$\tau^{-1} = \tau_{QTM}^{-1} + CT^n + \tau_0^{-1} \exp(-U_{eff}/k_BT) \quad (1)$$

Compared to **1**, the QTM of **2** is apparently weaker, and thus the fitting of the $\ln(\tau)$ versus T^{-1} curves takes into account only the Orbach and Raman processes, as shown in eq 2.[16,26,29b] The fitting in the temperature between 11 and 58 K for complex **2** resulted in $\tau_0 = 1.5 \times 10^{-12}$ s, U_{eff}/k_B = 1149.7 K, $C = 1.8 \times 10^{-4}$ $s^{-1}\cdot K^{-3.5}$, and n = 3.5.

$$\tau^{-1} = CT^n + \tau_0^{-1} \exp(-U_{eff}/k_BT) \quad (2)$$

According to ab initio calculations (see the Supporting Information for the details), the transversal g factor, i.e., g_{XY}, of the ground-state Kramers doublet of **2** (0.98×10^{-3}) is clearly smaller than that of **1** (0.23×10^{-2}). In general, the QTM rate scales approximately to g_{XY}^2. Thus, ab initio calculations confirmed the fact that the QTM of **2** is apparently weaker than that of **1**. In the aspect of U_{eff}, on the basis of ab initio results (Figure S16 and Tables S9 and S10), a recent theoretical method[32] provides the results of 944.0 and 1158.0 K for **1** and **2**, respectively. Apparently, theoretical values of U_{eff} show good consistency with the results of experimental fittings. Compared to the previous complexes in Tong's work,[17a] the ab initio results also indicate that the complexes here possess similar strengths of QTM but larger crystal-field splittings. Furthermore, the atomic charges (in lel) and electrostatic potentials from ab initio calculations for the complexes (Tables S11 and S12) indicate that the equatorial pyridyl N atoms of the complexes in this work have obviously smaller values of the negative charge, which is obviously due to the electron-withdrawing group on the equatorial plane of the ligand. Therefore, we tentatively consider that this is the main influencing factor for the increasing temperature of the open hysteresis loops of the complexes here.

In summary, we have successfully obtained two mononuclear Dy^{III} complexes **1** and **2**, which exhibit relaxation barriers of up to 837.7 and 1149.7 K and open hysteresis loops of up to ca. 20 and 30 K, respectively. Compared to Tong's complexes, the electron-withdrawing group modified to the ligand weakens the equatorial electrostatic field of the central Dy^{III} ion. This modification results into similar strengths of QTM but larger crystal-field splittings and, eventually, higher hysteresis temperatures of the systems here. This result may provide an effective approach to building more high-performance Dy^{III}-SMMs.

■ ASSOCIATED CONTENT

Supporting Information

The Supporting Information is available free of charge at https://pubs.acs.org/doi/10.1021/acs.inorgchem.0c01716.

Additional figures, X-ray crystallographic data and figures, selected bond lengths and angles, magnetic measurements, and theoretical calculations (PDF)

Accession Codes

CCDC 1999918 and 1999919 contain the supplementary crystallographic data for this paper. These data can be obtained free of charge via www.ccdc.cam.ac.uk/data_request/cif, or by emailing data_request@ccdc.cam.ac.uk, or by contacting The Cambridge Crystallographic Data Centre, 12 Union Road, Cambridge CB2 1EZ, UK; fax: +44 1223 336033.

https://dx.doi.org/10.1021/acs.inorgchem.0c01716
Inorg. Chem. XXXX, XXX, XXX−XXX

AUTHOR INFORMATION

Corresponding Authors

Bing Yin − *Key Laboratory of Synthetic and Natural Functional Molecule of the Ministry of Education, College of Chemistry and Materials Science, Northwest University, Xi'an 710127, P. R. China*; orcid.org/0000-0001-8668-9504; Email: rayinyin@nwu.edu.cn

Dongfeng Li − *Key Laboratory of Pesticide & Chemical Biology, Ministry of Education, College of Chemistry, Central China Normal University, Wuhan 430079, P. R. China*; orcid.org/0000-0001-6537-3279; Email: dfli@mail.ccnu.edu.cn

Authors

Li Zhu − *Key Laboratory of Pesticide & Chemical Biology, Ministry of Education, College of Chemistry, Central China Normal University, Wuhan 430079, P. R. China*

Pengtao Ma − *Henan Key Laboratory of Polyoxometalate Chemistry, College of Chemistry and Chemical Engineering, Henan University, Kaifeng, Henan 475004, P. R. China*

Complete contact information is available at: https://pubs.acs.org/10.1021/acs.inorgchem.0c01716

Notes

The authors declare no competing financial interest.

ACKNOWLEDGMENTS

We are thankful for financial support from the National Natural Science Foundation of China (Grants 21771074 and 21103137) and the computational resources from the chemical high-performance computing center of Northwest University. B.Y. is thankful for a fellowship grant under the "Excellent Young Scholar Plan" (Grant 338050094) from Northwest University.

REFERENCES

(1) (a) Leuenberger, M. N.; Loss, D. Quantum computing in molecular magnets. *Nature* **2001**, *410*, 789−793. (b) Thiele, S.; Balestro, F.; Ballou, R.; Klyatskaya, S.; Ruben, M.; Wernsdorfer, W. Electrically driven nuclear spin resonance in single-molecule magnets. *Science* **2014**, *344*, 1135−1138. (c) Gatteschi, D.; Sessoli, R. Quantum tunneling of magnetization and related phenomena in molecular materials. *Angew. Chem., Int. Ed.* **2003**, *42*, 268−297.

(2) (a) Bogani, L.; Wernsdorfer, W. Molecular spintronics using single-molecule magnets. *Nat. Mater.* **2008**, *7*, 179−186. (b) Vincent, R.; Klyatskaya, S.; Ruben, M.; Wernsdorfer, W.; Balestro, F. Electronic read-out of a single nuclear spin using a molecular spin transistor. *Nature* **2012**, *488*, 357−360.

(3) (a) Mannini, M.; Pineider, F.; Sainctavit, P.; Danieli, C.; Otero, E.; Sciancalepore, C.; Talarico, A. M.; Arrio, M. A.; Cornia, A.; Gatteschi, D.; Sessoli, R. Magnetic memory of a single-molecule quantum magnet wired to a gold surface. *Nat. Mater.* **2009**, *8*, 194. (b) Urdampilleta, M.; Klyatskaya, S.; Cleuziou, J. P.; Ruben, M.; Wernsdorfer, W. Magnetic interaction between a radical spin and a single-molecule magnet in a molecular spin-valve. *Nat. Mater.* **2011**, *10*, 502−506.

(4) (a) Blagg, R. J.; Ungur, L.; Tuna, F.; Speak, J.; Comar, P.; Collison, D.; Wernsdorfer, W.; McInnes, E. J. L.; Chibotaru, L. F.; Winpenny, R. E. P. Magnetic relaxation pathways in lanthanide single-molecule magnets. *Nat. Chem.* **2013**, *5*, 673−678. (b) Ungur, L.; Le Roy, J. J.; Korobkov, I.; Murugesu, M.; Chibotaru, L. F. Fine-tuning the local symmetry to attain record blocking temperature and magnetic remanence in a single-ion magnet. *Angew. Chem., Int. Ed.* **2014**, *53*, 4413−4417. (c) Gupta, S. K.; Rajeshkumar, T.; Rajaraman, G.; Murugavel, R. An air-stable Dy(III) single-ion magnet with high anisotropy barrier and blocking temperature. *Chem. Sci.* **2016**, *7*, 5181−5191. (d) Huang, W.; Shen, F. X.; Wu, S. Q.; Liu, L.; Wu, D. Y.; Zheng, Z.; Xu, J.; Zhang, M.; Huang, X. C.; Jiang, J.; Pan, F. F.; Li, Y.; Zhu, K.; Sato, O. Metallogrid Single-molecule magnet: solvent-induced nuclearity transformation and magnetic hysteresis at 16 K. *Inorg. Chem.* **2016**, *55*, 5476−5484.

(5) (a) Gonidec, M.; Biagi, R.; Corradini, V.; Moro, F.; De Renzi, V.; del Pennino, U.; Summa, D.; Muccioli, L.; Zannoni, C.; Amabilino, D. B.; Veciana, J. Surface supramolecular organization of a terbium(III) double-decker complex on graphite and its single molecule magnet behavior. *J. Am. Chem. Soc.* **2011**, *133*, 6603−6612. (b) Zhang, P.; Guo, Y. N.; Tang, J. K. Recent advances in dysprosium-based single molecule magnets: structural overview and synthetic strategies. *Coord. Chem. Rev.* **2013**, *257*, 1728−1763. (c) Woodruff, D. N.; Winpenny, R. E. P.; Layfield, R. A. Lanthanide single-molecule magnets. *Chem. Rev.* **2013**, *113*, 5110−5148. (d) Sessoli, R.; Powell, A. K. Strategies towards single molecule magnets based on lanthanide ions. *Coord. Chem. Rev.* **2009**, *253*, 2328−2341. (e) Chilton, N. F.; Goodwin, C. A.; Mills, D. P.; Winpenny, R. E. The first near-linear bis(amide) f-block complex: a blueprint for a high temperature single molecule magnet. *Chem. Commun.* **2015**, *51*, 101−103.

(6) (a) Sorace, L.; Benelli, C.; Gatteschi, D. Lanthanides in molecular magnetism: old tools in a new field. *Chem. Soc. Rev.* **2011**, *40*, 3092−3104. (b) Guo, Y. N.; Xu, G. F.; Guo, Y.; Tang, J. K. Relaxation dynamics of dysprosium(III) single molecule magnets. *Dalton Trans.* **2011**, *40*, 9953−9963. (c) Habib, F.; Murugesu, M. Lessons learned from dinuclear lanthanide nano-magnets. *Chem. Soc. Rev.* **2013**, *42*, 3278−3288.

(7) (a) Guo, F. S.; Day, B. M.; Chen, Y. C.; Tong, M. L.; Mansikkamäki, A.; Layfield, R. A. A dysprosium metallocene single-molecule magnet functioning at the axial limit. *Angew. Chem., Int. Ed.* **2017**, *56*, 11445−11449. (b) Guo, F. S.; Day, B. M.; Chen, Y. C.; Tong, M. L.; Mansikkamäki, A.; Layfield, R. A. Magnetic hysteresis up to 80 K in a dysprosium metallocene single-molecule magnet. *Science* **2018**, *362*, 1400−1403.

(8) Chen, Z. L.; Yu, S.; Wang, R. D.; Li, B.; Yin, B.; Liu, D. C.; Liang, Y. N.; Yao, D.; Liang, F. P. Three Dy(III) single-ion magnets bearing the tropolone ligand: structure, magnetic properties and theoretical elucidation. *Dalton Trans.* **2019**, *48*, 6627−6637. (b) Zou, H. H.; Meng, T.; Chen, Q.; Zhang, Y. Q.; Wang, H. L.; Li, B.; Wang, K.; Chen, Z. L.; Liang, F. P. Bifunctional Mononuclear Dysprosium Complexes: Single-Ion Magnet Behaviors and Antitumor Activities. *Inorg. Chem.* **2019**, *58*, 2286−2298. (c) Yu, S.; Chen, Z. L.; Hu, H. C.; Li, Bo.; Liang, Y. N.; Liu, D. C.; Zou, H. H.; Yao, D.; Liang, F. P. Two mononuclear dysprosium(III) complexes with their slow magnetic relaxation behaviors tuned by coordination geometry. *Dalton Trans.* **2019**, *48*, 16679−16686.

(9) (a) Gregson, M.; Chilton, N. F.; Ariciu, A. M.; Tuna, F.; Crowe, I. F.; Lewis, W.; Blake, A. J.; Collison, D.; McInnes, E. J. L.; Winpenny, R. E. P.; Liddle, S. T. A monometallic lanthanide bis(methanediide) single molecule magnet with a large energy barrier and complex spin relaxation behaviour. *Chem. Sci.* **2016**, *7*, 155−165. (b) Huang, G.; Fernandez-Garcia, G.; Badiane, I.; Camarra, M.; Freslon, S.; Guillou, O.; Daiguebonne, C.; Totti, F.; Cador, O.; Guizouarn, T.; Le Guennic, B.; Bernot, K. Magnetic slow relaxation in a metal-organic framework made of chains of ferromagnetically coupled single-molecule magnets. *Chem. - Eur. J.* **2018**, *24*, 6983−6991. (c) Briganti, M.; Garcia, G. F.; Jung, J. L.; Sessoli, R.; Le Guennic, B.; Totti, F. Covalency and magnetic anisotropy in lanthanide single molecule magnets: the DyDOTA archetype. *Chem. Sci.* **2019**, *10*, 7233−7245.

(10) Li, J.; Gómez-Coca, S.; Dolinar, B. S.; Yang, L.; Yu, F.; Kong, M.; Zhang, Y. Q.; Song, Y.; Dunbar, K. R. Hexagonal bipyramidal Dy(III) complexes as a structural archetype for single-molecule magnets. *Inorg. Chem.* **2019**, *58*, 2610−2617.

(11) Randall McClain, K.; Gould, C. A.; Chakarawet, K.; Teat, S. J.; Groshens, T. J.; Long, J. R.; Harvey, B. G. High-temperature magnetic blocking and magneto-structural correlations in a series of dysprosium(III) metallocenium single-molecule magnets. *Chem. Sci.* **2018**, *9*, 8492−8503.

(12) Pugh, T.; Vieru, V.; Chibotaru, L. F.; Layfield, R. A. Magneto-structural correlations in arsenic- and selenium-ligated dysprosium single-molecule magnets. *Chem. Sci.* **2016**, *7*, 2128−2137.
(13) (a) Goodwin, C. A. P.; Ortu, F.; Reta, D.; Chilton, N. F.; Mills, D. P. Molecular magnetic hysteresis at 60 K in dysprosocenium. *Nature* **2017**, *548*, 439−442. (b) Evans, P.; Reta, D.; Whitehead, G. F. S.; Chilton, N. F.; Mills, D. P. Bis-monophospholyl dysprosium cation showing magnetic hysteresis at 48 K. *J. Am. Chem. Soc.* **2019**, *141*, 19935−19940.
(14) Al Hareri, M.; Gavey, E. L.; Regier, J.; Ras Ali, Z.; Carlos, L. D.; Ferreira, R. A. S.; Pilkington, M. Encapsulation of a $[Dy(OH_2)_8]^{3+}$ cation: magneto-optical and theoretical studies of a caged, emissive SMM. *Chem. Commun.* **2016**, *52*, 11335−11338.
(15) Ungur, L.; Chibotaru, L. F. Strategies toward high-temperature lanthanide-based single molecule magnets. *Inorg. Chem.* **2016**, *55*, 10043−10056.
(16) Canaj, A. B.; Singh, M. K.; Regincós Marti, E.; Damjanovic, M.; Wilson, C.; Cespedes, O.; Wernsdorfer, W.; Rajaraman, G.; Murrie, M. Boosting axiality in stable high-coordinate Dy(III) single-molecule magnets. *Chem. Commun.* **2019**, *55*, 5950−5953.
(17) (a) Liu, J.; Chen, Y. C.; Liu, J. L.; Vieru, V.; Ungur, L.; Jia, J. H.; Chibotaru, L. F.; Lan, Y.; Wernsdorfer, W.; Gao, S.; Chen, X. M.; Tong, M. L. A stable pentagonal bipyramidal Dy(III) single-ion magnet with a record magnetization reversal barrier over 1000 K. *J. Am. Chem. Soc.* **2016**, *138*, 5441−5450. (b) Chen, Y. C.; Liu, J. L.; Ungur, L.; Liu, J.; Li, Q. W.; Wang, L. F.; Ni, Z. P.; Chibotaru, L. F.; Chen, X. M.; Tong, M. L. Symmetry-supported magnetic blocking at 20 K in pentagonal bipyramidal Dy(III) single-ion magnets. *J. Am. Chem. Soc.* **2016**, *138*, 2829−2837. (c) Liu, J. L.; Chen, Y. C.; Zheng, Y. Z.; Lin, W. Q.; Ungur, L.; Wernsdorfer, W.; Chibotaru, L. F.; Tong, M. L. Switching the anisotropy barrier of a single-ion magnet by symmetry change from quasi-D_{5h} to quasi-O_h. *Chem. Sci.* **2013**, *4*, 3310−3316. (d) Huang, G. Z.; Ruan, Z. Y.; Zheng, J. Y.; Chen, Y. C.; Wu, S. G.; Liu, J. L.; Tong, M. L. Seeking magneto-structural correlations in easily tailored pentagonal bipyramid Dy(III) single-ion magnets. *Sci. China: Chem.* **2020**, *63*, 1066−1074.
(18) (a) Ding, Y. S.; Chilton, N. F.; Winpenny, R. E. P.; Zheng, Y. Z. On approaching the limit of molecular magnetic anisotropy: A near-perfect pentagonal bipyramidal dysprosium(III) single-molecule magnet. *Angew. Chem., Int. Ed.* **2016**, *55*, 16071−16074. (b) Ding, Y. S.; Han, T.; Zhai, Y. Q.; Reta, D.; Chilton, N. F.; Winpenny, R. E. P.; Zheng, Y. Z. A study of magnetic relaxation in dysprosium(III) single molecule magnets. *Chem. - Eur. J.* **2020**, *26*, 5893. (c) Yu, K. X.; Kragskow, J. G. C.; Ding, Y. S.; Zhai, Y. Q.; Reta, D.; Chilton, N. F.; Zheng, Y. Z. Enhancing Magnetic Hysteresis in Single-Molecule Magnets by Ligand Functionalization. *Chem.* **2020**, *6*, 1777.
(19) (a) Jiang, Z. J.; Sun, L.; Yang, Q.; Yin, B.; Ke, H. S.; Han, J.; Wei, Q.; Xie, G.; Chen, S. P. Excess axial electrostatic repulsion as a criterion for pentagonal bipyramidal Dy^{III} single-ion magnets with high U_{eff} and T_B. *J. Mater. Chem. C* **2018**, *6*, 4273−4280. (b) Li, M.; Wu, H.; Yang, Q.; Ke, H.; Yin, B.; Shi, Q.; Wang, W.; Wei, Q.; Xie, G.; Chen, S. P. Experimental and theoretical interpretation on the magnetic behavior in a series of pentagonal-bipyramidal Dy^{III} single-ion magnets. *Chem. - Eur. J.* **2017**, *23*, 17775−17787.
(20) Gupta, S. K.; Rajeshkumar, T.; Rajaraman, G.; Murugavel, R. An air-stable Dy(III) single-ion magnet with high anisotropy barrier and blocking temperature. *Chem. Sci.* **2016**, *7*, 5181−5191.
(21) Bar, A. K.; Kalita, P.; Sutter, J. P.; Chandrasekhar, V. Pentagonal-bipyramid Ln(III) complexes exhibiting single-ion magnet behavior: a rational synthetic approach for a rigid equatorial plane. *Inorg. Chem.* **2018**, *57*, 2398−2401.
(22) (a) Guo, Y. N.; Xu, G. F.; Wernsdorfer, W.; Ungur, L.; Guo, Y.; Tang, J. K.; Zhang, H. J.; Chibotaru, L. F.; Powell, A. K. Strong axiality and Ising exchange interaction suppress zero-field tunneling of magnetization of an asymmetric Dy_2 single-molecule magnet. *J. Am. Chem. Soc.* **2011**, *133*, 11948−11951. (b) Tang, J. K.; Hewitt, I.; Madhu, N. T.; Chastanet, G.; Wernsdorfer, W.; Anson, C. E.; Benelli, C.; Sessoli, R.; Powell, A. K. Dysprosium triangles showing single-molecule magnet behavior of thermally excited spin state. *Angew. Chem., Int. Ed.* **2006**, *45*, 1729−1733. (c) Tian, H.; Zhao, L.; Guo, Y. N.; Guo, Y.; Tang, J. K.; Liu, Z. Quadruple-CO_3^{2-} bridged octanuclear dysprosium(III) compound showing single-molecule magnet behaviour. *Chem. Commun.* **2012**, *48*, 708−710.
(23) Ungur, L.; Chibotaru, L. F. Magnetic anisotropy in the excited states of low symmetry lanthanide complexes. *Phys. Chem. Chem. Phys.* **2011**, *13*, 20086−20090.
(24) Dong, H. M.; Li, H. Y.; Zhang, Y. Q.; Yang, E. C.; Zhao, X. J. Magnetic relaxation dynamics of a centrosymmetric Dy_2 single molecule magnet triggered by magnetic-site dilution and external magnetic field. *Inorg. Chem.* **2017**, *56*, 5611−5622.
(25) Liu, J. L.; Chen, Y. C.; Tong, M. L. Symmetry strategies for high performance lanthanide-based single-molecule magnets. *Chem. Soc. Rev.* **2018**, *47*, 2431−2453.
(26) Liddle, S. T.; van Slageren, J. Improving f-element single molecule magnets. *Chem. Soc. Rev.* **2015**, *44*, 6655−6669.
(27) Ishikawa, N.; Sugita, M.; Ishikawa, T.; Koshihara, S. Y.; Kaizu, Y. Lanthanide double-decker complexes functioning as magnets at the single-molecular level. *J. Am. Chem. Soc.* **2003**, *125*, 8694−8695.
(28) (a) Pedersen, K. S.; Ungur, L.; Sigrist, M.; Sundt, A.; Schau-Magnussen, M.; Vieru, V.; Mutka, H.; Rols, S.; Weihe, H.; Waldmann, O.; Chibotaru, L. F.; Bendix, J.; Dreiser, J. Modifying the properties of 4f single-ion magnets by peripheral ligand functionalisation. *Chem. Sci.* **2014**, *5*, 1650−1660. (b) Le Roy, J. J.; Ungur, L.; Korobkov, I.; Chibotaru, L. F.; Murugesu, M. Coupling strategies to enhance single-molecule magnet properties of erbium-cyclooctatetraenyl complexes. *J. Am. Chem. Soc.* **2014**, *136*, 8003−8010.
(29) (a) Huang, G. Z.; Ruan, Z. Y.; Zheng, J. Y.; Wu, J. Y.; Chen, Y. C.; Li, Q. W.; Akhtar, M. N.; Liu, J. L.; Tong, M. L. Enhancing single-molecule magnet behavior of linear Co^{II}-Dy^{III}-Co^{II} complex by introducing bulky diamagnetic moiety. *Sci. China: Chem.* **2018**, *61*, 1399−1404. (b) Chen, Y. C.; Liu, J. L.; Wernsdorfer, W.; Liu, D.; Chibotaru, L. F.; Chen, X. M.; Tong, M. L. Hyperfine-interaction-driven suppression of quantum tunneling at zero field in a holmium(III) single-ion magnet. *Angew. Chem., Int. Ed.* **2017**, *56*, 4996−5000.
(30) Osa, S.; Kido, T.; Matsumoto, N.; Re, N.; Pochaba, A.; Mrozinski, J. A tetranuclear 3d-4f single molecule magnet: $[Cu^{II}LTb^{III}(hfac)_2]_2$. *J. Am. Chem. Soc.* **2004**, *126*, 420−421.
(31) Das, C.; Upadhyay, A.; Shanmugam, M. Influence of radicals on magnetization relaxation dynamics of pseudo-octahedral lanthanide iminopyridyl complexes. *Inorg. Chem.* **2018**, *57*, 9002−9011.
(32) Yin, B.; Li, C. A method to predict both relaxation time of quantum tunneling of magnetization and effective barrier of magnetic reversal for Kramers single-ion magnet. *Phys. Chem. Chem. Phys.* **2020**, *22*, 9923−9933.

https://dx.doi.org/10.1021/acs.inorgchem.0c01716
Inorg. Chem. XXXX, XXX, XXX−XXX